Since January 2020 Elsevier has created a COVID-19 resource centre with free information in English and Mandarin on the novel coronavirus COVID-19. The COVID-19 resource centre is hosted on Elsevier Connect, the company's public news and information website.

Journal of Hospital Infection 106 (2020) 649–656

Available online at www.sciencedirect.com

Journal of Hospital Infection

journal homepage: www.elsevier.com/locate/jhin

A cold water, ultrasonically activated stream efficiently removes proteins and prion-associated amyloid from surgical stainless steel

T.J. Secker [a,*], T.G. Leighton [b,c], D.G. Offin [d], P.R. Birkin [d], R.C. Hervé [a], C.W. Keevil [a]

[a] Environmental Healthcare Unit, School of Biological Sciences, Faculty of Environmental and Life Sciences, University of Southampton, Southampton, UK
[b] Institute of Sound and Vibration Research, Faculty of Engineering and Environment, University of Southampton, Southampton, UK
[c] Sloan Water Technology Ltd, Chilworth, Southampton, UK
[d] Chemistry, Faculty of Environmental and Life Sciences, University of Southampton, Southampton, UK

ARTICLE INFO

Article history:
Received 7 July 2020
Accepted 11 September 2020
Available online 19 September 2020

Keywords:
Surgical
Protein
Prion
Decontamination
Ultrasonic cleaning
Creutzfeldt–Jakob disease

SUMMARY

Background: Sterile service department decontamination procedures for surgical instruments struggle to demonstrate efficient removal of the hardiest infectious contaminants, such as prion proteins. A recently designed novel system, which uses a low pressure ultrasonically activated, cold water stream, has previously demonstrated efficient hard surface cleaning of several biological contaminants.
Aim: To test the efficacy of an ultrasonically activated stream for the removal of tissue proteins, including prion-associated amyloid, from surgical stainless steel surfaces.
Methods: Test surfaces were contaminated with 22L, ME7 or 263K prion-infected brain homogenates. The surfaces were treated with the ultrasonically activated water stream for contact times of 5 and 10 s. Residual proteinaceous and amyloid contamination were quantified using sensitive microscopic analysis, and immunoblotting was used to characterize the eluted prion residues before and after treatment with the ultrasonically activated stream.
Findings: Efficient removal of the different prion strains from the surgical stainless steel surfaces was observed, and reduced levels of protease-susceptible and -resistant prion protein was detected in recovered supernatant.
Conclusion: This study demonstrated that an ultrasonically activated stream has the potential to be a cost-effective solution to improve current decontamination practices and has the potential to reduce hospital-acquired infections.

Introduction

At present, the reprocessing of surgical instruments uses a pre-wash, washer–disinfector cycle (run at elevated

* Corresponding author. Address: Environmental Healthcare Unit, School of Biological Sciences, Faculty of Environmental and Life Sciences, Building 85, University of Southampton, Southampton SO17 1BJ, UK. Tel.: +44 (0)2380.592034.
E-mail address: tjs1x07@soton.ac.uk (T.J. Secker).

https://doi.org/10.1016/j.jhin.2020.09.021
0195-6701/

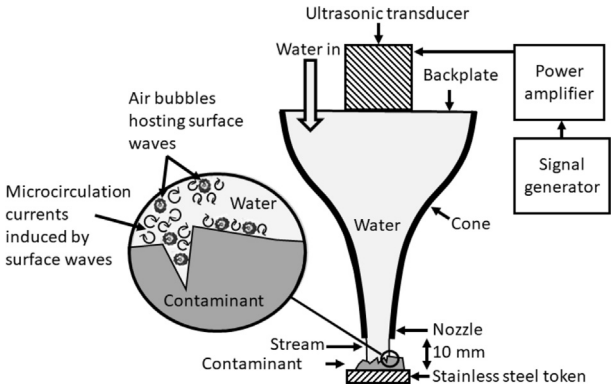

Figure 1. Schematic demonstrating the decontamination of a prion-inoculated surgical grade stainless-steel token by an ultrasonically activated stream nozzle. The inset magnifies a region on the prion contaminant where microscopic air bubbles, their walls rippling with ultrasonically excited surface waves, clean away the contaminant using microcirculation currents induced by these surface waves. (Adapted from Malakoutikhah *et al.* [46].)

temperature with detergents), and sterilization in high heat/pressure autoclaves [1]. Decontamination protocols for reusable surgical instruments are very efficient against microbiological contaminants. However, highly hydrophobic proteins such as prions, responsible for the transmission of variant Creutzfeldt—Jakob disease (vCJD), are readily adsorbed to surgical stainless-steel surfaces and poorly removed or inactivated by current decontamination methods. This results in an impending risk of iatrogenic transmission of vCJD [2—5]. This risk has been experimentally demonstrated in both animal and cell-based bioassays [6—9].

The latest estimated prevalence of asymptomatic carriers of the causative protein of vCJD (PrP^{Sc}) in the UK is approximately 1/2000 [10]. Whereas the full impact of the genetic susceptibility of the host remains unclear, the ostensibly long incubation periods and the potential for disease transmission via infected blood imply that all surgical procedures pose a risk of vCJD transmission [11—13].

Improvements in the methodologies used for reprocessing surgical instruments, potentially contaminated with prions, are required to diminish the risk of iatrogenic vCJD transmission. Novel, specialized prion decontamination protocols have been developed and in some cases marketed for sterile service departments (SSDs) [7,14—22]. However, some of these protocols are very aggressive and can be damaging to instrument surfaces and/or the washer—disinfectors themselves [14]. Simple methods to adopt into SSDs have been researched and demonstrated improved efficiency over current practices, such as preventing instruments from drying once contaminated, i.e. keeping them in a moist environment prior to cleaning [23—27].

Ultrasonic baths, commonly used for surface decontamination, come with drawbacks: they cannot contain instruments bigger than themselves, they pose difficulties in being taken to an instrument to 'clean-in-place', the instruments to be cleaned sit in a soup of previously removed contaminants, and (perhaps most importantly) the placement of objects in the tank can disturb the sound-field, producing cold (no sound) spots which can cause significantly reduced and sporadic cleaning efficacy [28]. Furthermore, ultrasonic cleaning baths operate by so-called inertial cavitation, whereby ultrasound violently collapses small gas bubbles in the liquid so that close to the bubble they generate high pressures (e.g. 2 GPa) [29,30]. Such collapses will damage susceptible materials. We know that ultrasonic cleaning baths generate pitting through inertial cavitation events that produce erosion. Since the 1960s, a standard method for measuring the effectiveness of an ultrasonic cleaning bath is to examine metal foil for pitting [31—33]. Another is to monitor the mass loss that the ultrasonic bath produces in a metal block [32—34].

One issue for contamination is that cavitation erosion mass loss can result in the formation of micro-scale crevices and pits, which can make subsequent cleaning of a reusable instrument more difficult. The 'mark 1' UAS system tested here cleans by use of such convection, resulting from surface waves on the bubble wall, and this has been shown, through optical microscopic examination of the surfaces tested here, not to cause detectable damage. This innovation stimulates such surface waves on the walls of non-inertial bubbles in a stream of mains tap water, flowing at ~2 L per minute and generating only non-inertial cavitation on the surface to be cleaned [35]. With ultrasonically activated stream (UAS) technology (Figure 1), bubbles do not collapse as they would during inertial cavitation, but instead, the ultrasound stimulates rapid surface waves that oscillate on the bubble wall, generating a gentle scrubbing action [36]. This phenomenon has been demonstrated to be effective at removing contamination from hands, skin, proteins from stainless steel and tissue from bone grafts, dental biofilms, marine biofouling, and contaiminant from railtracks [37—42]. Bjerknes forces aid the scrubbing bubbles in efficiently removing contaminants from microscopic crevices, such as those found on worn surgical instruments, that are traditionally difficult to clean by brushes, wiping, or by chemical means that rely on passive diffusion for reagents to penetrate deep into the crevice [43—45]. The efficient removal of contamination from crevices using a UAS system has been demonstrated previously [40]. Furthermore, the microstreaming that radiates from the resonating bubbles can penetrate into crevices present on the surfaces of the contaminant as shown in the insert in Figure 1 [46].

The fact that such results can be obtained in cold water without chemical additives warrants investigation of UAS for the removal of infectious prion proteins from surgical surfaces. High temperature decontamination using aggressive enzymatic or alkaline solutions, that are currently adopted to clean expensive surgical items (such as intricate neurosurgical tools), are ineffective at protein and prion removal, and can shorten the surgical item lifetime [47]. It is not the purpose of this study to explore the replacement of such standard cleaning practices. However, given the above properties of UAS, it is important to explore the possible benefits of including an innovative cold water UAS pre-wash (at the stage where SSDs conduct hand-brushing of instruments under a stream of water) that can be introduced with minimal operator training. This would be particularly beneficial if it could be conducted immediately after instrument use (e.g. before contaminated tissue dries on the instrument and becomes harder to remove), although in this trial the contaminant is tested in a dried-on state. The question is whether such a UAS pre-wash could remove a substantial proportion of the contaminant, especially from microscopic crevices of the type associated with worn surgical instrument surfaces, and break up aggregates in which the inner portion of biological contaminant is partially protected from subsequent enzymatic cleaning chemistries.

A previous study demonstrated efficient tissue protein removal from surgical stainless steel using the UAS [39]. However, due to the globular nature of the predominantly β-sheet-structured infectious prion protein, it adheres to surgical stainless steel far more rigorously than do normal brain tissue proteins, and therefore the ability of UAS to remove brain tissue protein cannot be taken as an indicator of any efficacy in reducing the iatrogenic transmission risk of vCJD. Therefore, this study involved the contamination of surgical stainless-steel surfaces with several amyloid-rich brain homogenates from prion-infected rodents. Normal tissue proteins and more hazardous prion-associated amyloid were differentially stained and analysed using sensitive in-situ microscopy, to compare the ability of UAS to remove both during the same cleaning operation.

Methods

Token preparation

Unpolished (average roughness (R_a) ~0.25 μm, comparable to the average roughness associated with surgical instrument surfaces) surgical grade stainless-steel tokens (316L grade, 10 mm × 30 mm) were used throughout all the protein experiments [48]. Prior to inoculating, tokens were decontaminated and analysed to be deemed free of any contamination following a previously described protocol [49].

Brain homogenate preparation

Murine scrapie ME7-infected brain homogenate produced from C57BL mice (TSE Resource Centre, Roslin Institute, University of Edinburgh, UK), murine scrapie 22L-infected brain homogenate produced from C57BL/6J mice (kindly donated from the Neuroscience Department, School of Biological Sciences, University of Southampton), and Syrian hamster scrapie 263K-infected brain homogenates (TSE Resource Centre, Roslin Institute, University of Edinburgh, UK) were standardized to 1 mg/mL (BSA equivalent) in phosphate-buffered saline (PBS; Gibco, Waltham, MA, USA) with 0.1% (v/v) Tween 20 (Sigma–Aldrich, St Louis, MO, USA) as previously described [50].

Token contamination and cleaning using ultrasonically activated stream (UAS)

Pristine tokens were spiked with 1 μL (1 μg BSA equivalent) drops of 22L-, ME7- or 263K-infected brain homogenate, and dried at 37°C for 2 h or room temperature for 24 h. Tokens were subjected to decontamination using a prototype recirculating UAS device (the Mark I StarStream® system (F0030001)) using fresh dH_2O for each sample, running at 2.32 ± 0.02 L/min at room temperature with the ultrasound on for 5 and 10 s contact times, with the sample being 10 mm from the nozzle (Figure 1). Once processed, the tokens were dried at 37°C for 1 h prior to staining and analysis.

Protein and prion-associated amyloid staining, visualization, and image analysis

Residual tissue protein and prion-associated amyloid on the control and processed surfaces was quantified, *in situ*, using the total protein blot stain SYPRO Ruby (SR; Invitrogen, Inchinnan, UK) and the amyloid-specific stain Thioflavin T (ThT (0.2% (w/v) in 0.01 M HCl); Sigma–Aldrich), as described elsewhere [50,51]. Fluorescent signal was visualized using episcopic differential interference contrast (EDIC) microscopy coupled with epifluorescence (Best Scientific, Wroughton, UK) [50,52]. Full X/Y scans of the contaminated areas were acquired at ×100 magnification showing the SYPRO Ruby (excitation: 470 nm; emission: 618 nm) and ThT (0.2% (w/v) in 0.01 M HCl; Sigma–Aldrich) signals. The captured images were analysed using ImageJ software (National Institutes of Health).

Protein filtration and immunoblot analysis

To analyse the effects of the UAS treatment on infectious prion proteins, immunoblot analysis was used to determine the presence of PrP^{C} and proteinase K (PK)-resistant PrP^{Sc} in both 22L-spiked distilled water, as an untreated control, and the effluent taken from the UAS system post cleaning of 22L-spiked stainless-steel tokens. Controls were prepared by spiking 1 L of sterile distilled water with 15 μg of 22L-infected brain homogenate. UAS-positive samples were prepared from capturing the 1 L UAS effluent post cleaning of 15 surgical stainless-steel tokens contaminated with 1 μg 22L-infected brain homogenates each (dried for 24 h at room temperature) as described above. The control and effluent solutions were filtered through nitrocellulose membranes to capture the suspended protein aggregates. Following replicate filtrations for each group, membranes were directly immunochemically stained and examined, or subjected to PK (Sigma–Aldrich) digestion at a final concentration of 10 ng per μg of total protein, for 30 min at 37°C. The PK digestion was halted by moving the samples to ice and the addition of Pefabloc (Sigma–Aldrich). All of the membranes were blocked by submersion in 5% (w/v) skimmed milk powder (Marvel) in PBS-T (PBS containing 0.1% (v/v) Tween 20; Sigma–Aldrich) for 1 h at room temperature. PrP was detected using the monoclonal antibody 6H4 (1/5000 (v/v) in PBS-T; Prionics, Zürich, Switzerland) for 1 h at room temperature followed by horseradish peroxidase-conjugated antimouse IgG secondary antibody (GE Healthcare, UK; 1/10,000 (v/v) in PBS-T) for 1 h at room temperature. The immunoreactive proteins were visualized using the enhanced chemiluminescence substrate (ECL plus; GE Healthcare, Amersham, UK) developed on X-ray film (Fuji Film, Bedford, UK).

Statistical analysis

One-way analysis of variance was used to compare the sample means, in each data set, for both the protein and prion-amyloid attachment to the stainless steel. The Games–Howell post-hoc test was used to compare the difference between the controls of each homogenate type (22L, 263K and ME7) and the two UAS contact times for each homogenate; $P \leq 0.05$ was considered significant.

Data availability

The datasets generated and analysed during this study are available from the University of Southampton repository at https://doi.org/10.5258/SOTON/.

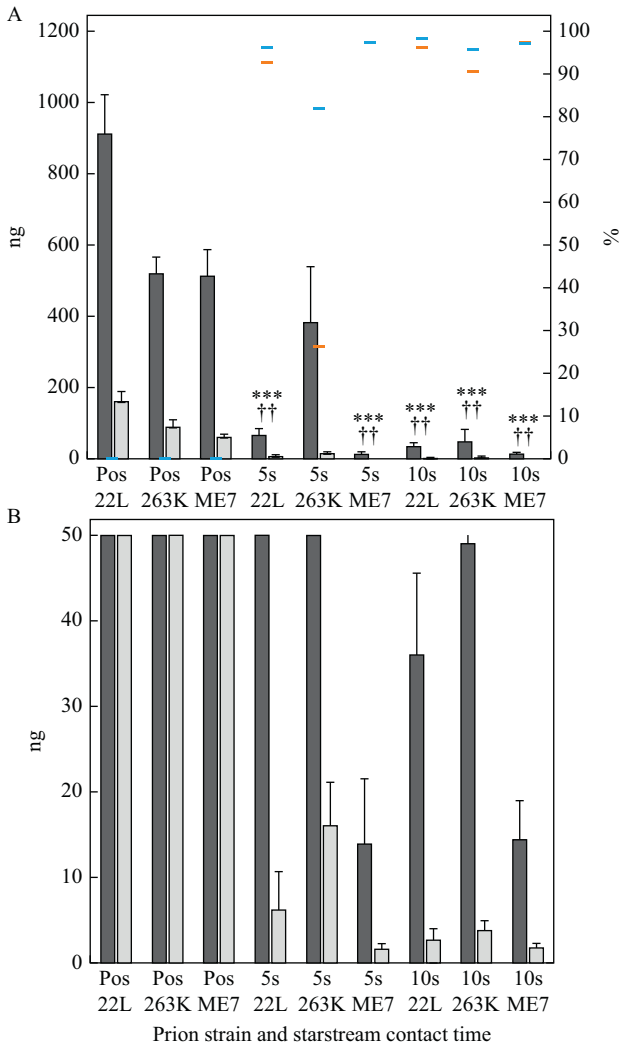

Figure 2. Tissue protein (dark grey bars) and prion-associated amyloid (light grey bars) attachment from different prion-infected brain homogenates (22L, ME7 and 263K) to surgical stainless steel pre and post treatment with an ultrasonically activated stream (A). Brain homogenate was initially dried for 2 h at 37°C prior to cleaning (Pos). The orange dashes represent percentage protein removal and the blue dashes represent percentage prion-associated amyloid removal (A). (B) Graph with expanded *y*-axis scale to distinguish the lower levels of contamination. Data are mean ± SEM ($N = 9$); however, in decontamination and other research areas, outliers are also important to assessing outcomes, whether it be risk of infection, or the response of the most sensitive individuals to some stimulus [53]. ***$P \leq 0.001$ for total proteins; ††$P \leq 0.01$ for amyloid, when compared to the corresponding positive controls, respectively.

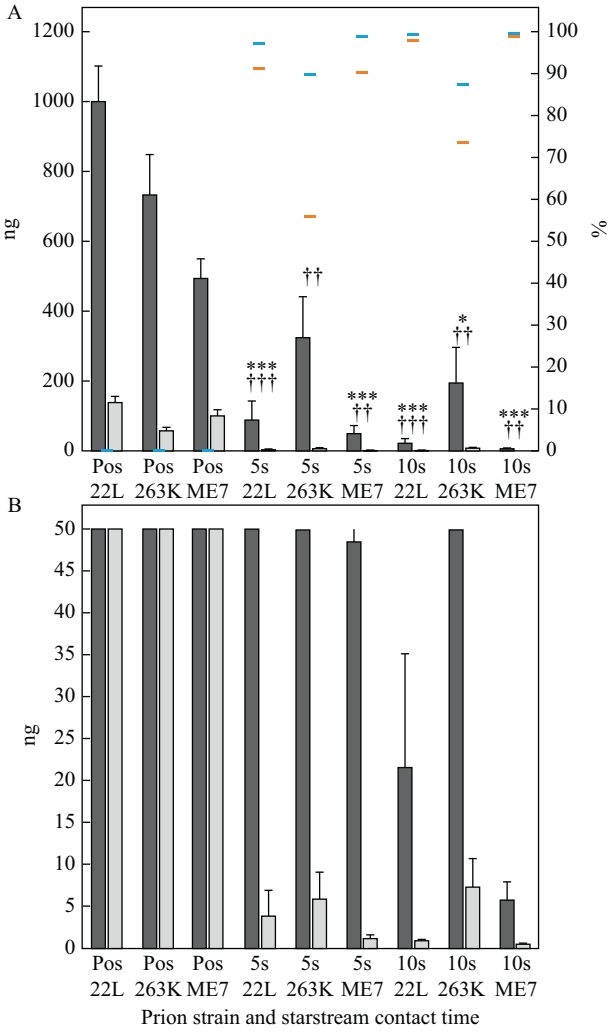

Figure 3. Tissue protein (dark grey bars) and prion-associated amyloid (light grey bars) attachment from different prion-infected brain homogenates (22L, ME7 and 263K) to surgical stainless steel pre and post treatment (5 and 10 s contact times) with an ultrasonically activated stream (A). Brain homogenate was initially dried for 24 h at room temperature prior to cleaning (Pos). The orange dashes represent percentage protein removal and the blue dashes represent percentage prion-associated amyloid removal (A). Graph B has an expanded *y*-axis scale to highlight the lower levels of contamination. Data are mean ± SEM ($N = 9$); however, in decontamination and other research areas, outliers are also important to assessing outcomes, whether it be risk of infection, or the response of the most sensitive individuals to some stimulus [53]. *$P \leq 0.05$ and ***$P \leq 0.001$ for total proteins; ††$P \leq 0.01$ and †††$P \leq 0.001$ for amyloid, when compared to the corresponding positive controls, respectively.

Results

UAS decontamination of surgical stainless steel

The efficacy of the UAS system was tested for the removal of tissue protein and prion-associated amyloid from three different prion strains after 2 h drying at 37°C and 24 h at room temperature. After 2 h drying the 22L brain homogenate demonstrated the highest affinity for the stainless steel with the highest attachment of protein and prion-associated amyloid observed. The 263K- and ME7-infected brain homogenates demonstrated similar attachment of protein and prion-associated amyloid (Figure 2). The removal of the 22L (93–96% protein and 96–98% amyloid removal, respectively)- and the ME7 (97% protein and amyloid removal)-infected brain homogenates was very efficient after both 5 s and 10 s UAS

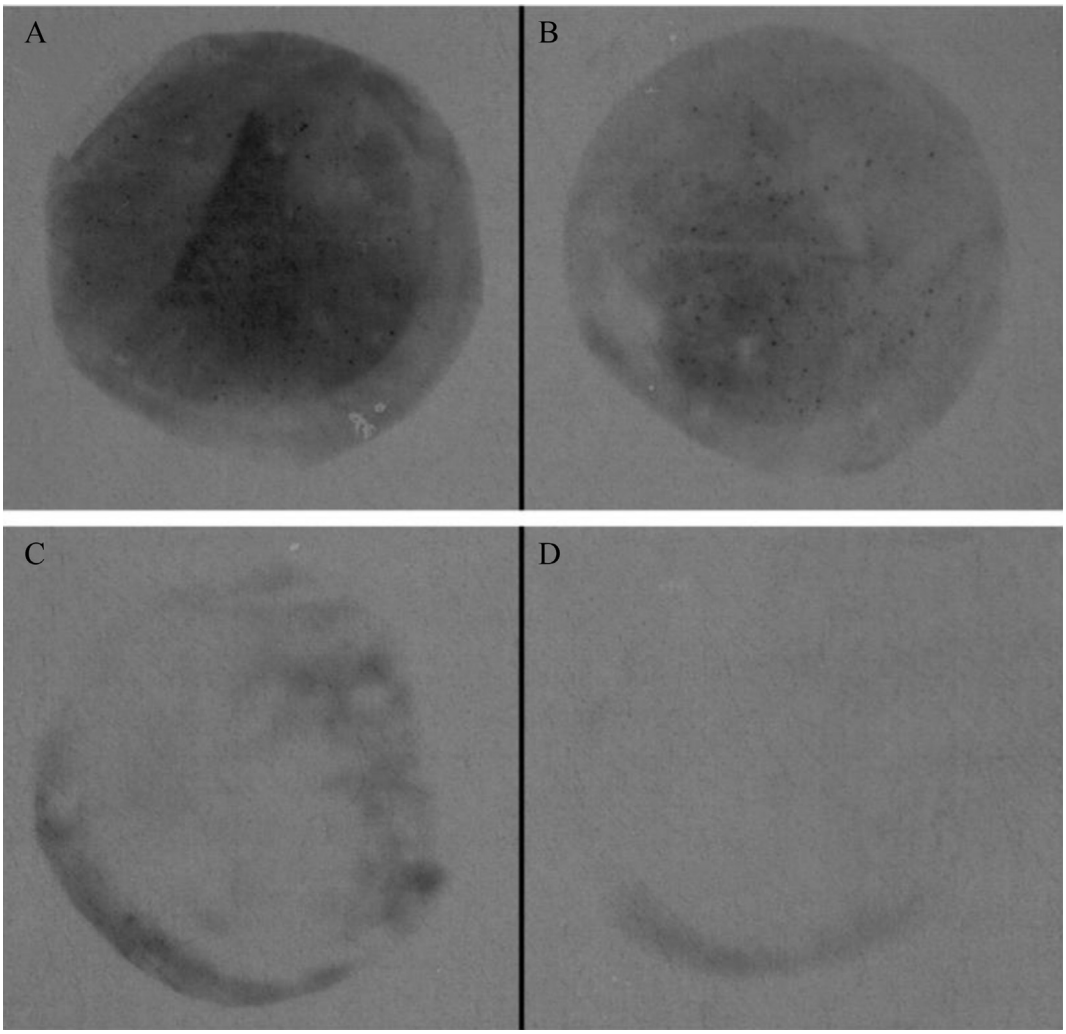

Figure 4. Immunoblot films showing captured proteins from 1 L of 22L-spiked solution containing 15 μg of 22 L homogenate in distilled water (A and B) and from the UAS system effluent after treating surfaces contaminated with the equivalent amount of 22L homogenate (C and D). Proteins were detected using the primary antibody 6H4, without (A and C) or with PK digestion (B and D).

treatment, respectively (Figure 2). The removal of 263K-infected homogenate required 10 s UAS treatment for effective removal with 26% protein and 82% amyloid removal after 5 s and 91% protein and 96% amyloid removal after 10 s UAS treatment (Figure 2). The percentage of amyloid within the total residual contamination was also very low, between 7% and 12% for all the samples after 10 s UAS treatment (Figure 2).

After 24 h drying at room temperature the 22L brain homogenate again demonstrated the highest affinity for the stainless steel with the highest attachment of protein and prion-associated amyloid observed. When compared with 2 h drying, the 263K-contaminated homogenate resulted in higher protein attachment after 24 h drying and the ME7-infected brain homogenates demonstrated similar protein attachment but higher prion-associated amyloid attachment (Figure 3). The removal of 22L and ME7 tissues was slightly more difficult using a 5 s UAS treatment with 91% and 90% protein and 97% and 99% amyloid removal, respectively (Figure 3). After 10 s UAS treatment, the removal was improved with 98% and 99% protein and 99% and 100% amyloid removal, respectively. The 263K was harder to remove after 24 h drying with only 56% protein and 90% amyloid removal after the 5 s UAS treatment; however, after the 10 s UAS treatment the cleaning was improved with 74% protein and 87% amyloid removal (Figure 3). The percentage of amyloid within the total residual contamination was again very low with 4–8% amyloid remaining for all the samples after 10 s UAS contact time (Figure 3).

Immunoblot analysis of residual PrP pre and post UAS cleaning

The effluent from the UAS system after decontaminating the 22L-spiked surfaces was filtered and labelled for residual prion protein (both non-resistant and PK-resistant) and compared to control samples of distilled water spiked with the equivalent amount of 22L brain homogenate. A clear reduction of both the PK-susceptible and -resistant prion protein from the tokens was observed (as demonstrated by the protein capture on nitrocellulose membranes following the previously demonstrated 98–99% protein and 99–100% amyloid removal, described above) after 10 s UAS treatment (Figure 4). The reduction in immunolabelled prion proteins post UAS treatment could be

demonstrating that the UAS treatment is destructive to the antibody-specific epitopes of the prion protein, therefore reducing the immunochemical detection post UAS treatment. Furthermore, small protein aggregates were observed in the control samples but not in the samples post UAS treatment, suggesting that the UAS may degrade and/or solubilize these aggregates.

In conclusion, current practices for the decontamination and sterilization of surgical instruments within SSDs are not entirely efficient at removing all potentially infectious material, especially, hardy prion proteins. Therefore, surgical instruments which may have come in contact with CJD-infected tissues cannot be deemed safe post cleaning and are subsequently quarantined [3,7,16,54]. Simple, cost-effective methods to prevent the initial attachment of bioburden to surgical surfaces have been demonstrated [25,27]. Ultrasonic baths provide efficient cleaning using water alone; however, the limitations associated with water baths have already been described in this article. This study has tested the efficacy of UAS technology for the removal of total protein and prion-amyloid from stainless steel, which is considered the most difficult contaminant to decontaminate in the surgical field.

The UAS technology demonstrated significant removal of the three prion strains tested after differing drying and UAS treatment times; however, increased UAS treatment times are required to further improve the efficacy of the UAS treatment. The efficient removal of ME7 and 22L, both murine-adapted scrapie strains, was very similar following both drying and UAS treatment times. However, 263K, a hamster-adapted scrapie strain, was harder to remove and would require a longer UAS treatment to reduce to the levels observed with the two murine strains. This observation suggests that the hamster brain constituents and PrP^{Sc} conformation are different from the mouse brains, showing increased affinity to stainless steel. This highlights the importance of studying different prion strains, from different hosts, when determining the efficacy of hospital decontamination tools. For comparison of the efficacy of the UAS system to that of cleaning chemistries used in SSDs, the removal of ME7-infected brain homogenate from stainless steel tokens using the same methodology as this study have been previously published [3,25]. Hervé *et al.* tested four different cleaning chemistries marketed for proteinaceous decontamination, demonstrating total protein removals of 39%, 97.9%, 98.9%, and 99.85%, respectively [3]. Secker *et al.* tested two cleaning chemistries, also marketed for proteinaceous decontamination, demonstrating total protein removal of zero and 90.1%, respectively [25]. All the cleaning chemistries tested in these studies required heating of the cleaning solution, whereas the UAS system tested here removed 97% total protein with cold water and only a 10 s contact time. A recent National Institute for Health Research Health Technology Assessment (HTA) has extensively compared studies quantifying the efficacy of interventions to reduce the surgical transmission of vCJD [55]. The other important observation was that the UAS system favourably removed the prion-associated amyloid (infectious prion proteins in the aggregated form) from the surfaces, demonstrated by the low percentages of the total residual proteinaceous contamination being ThT positive amyloid, compared to the comparative treatment using commercially available cleaning chemistries [3,25].

Immunoblot analysis of both PK-susceptible and -resistant residues of PrP was carried out to determine the presence and state of prion aggregates post UAS decontamination. Following the predetermined 98–99% protein and 99–100% prion-amyloid removal, described above, the supernatant from the UAS treatment was filtered and the prion proteins were labelled. The PK-resistant and -susceptible aggregates observed in the control immunoblots were not present in the UAS treated samples; this suggests that the UAS mechanism of action is causing the breakdown of the PrP aggregates, reducing the available epitopes for antibody binding, and therefore a reduction in antibody-positive PrP residues. Furthermore, this would explain why an increase in the removal of prion-amyloid using the UAS system was observed, as described earlier. Further work is required to confirm and determine whether the breakdown of PrP caused by the action of UAS correlates with a reduction in prion infectivity.

The results from this study demonstrated efficient removal of tissue proteins, and more importantly prion-associated amyloid from surgical stainless-steel harnessing the power of water at ambient temperature. Whereas the cleaning efficacy demonstrated by this system is improved compared to that of the best currently available cleaning chemistries tested on the same contaminants, the UAS appeared more effective at removing prion-amyloid as well as the total proteinaceous contamination.

This study has demonstrated the efficacious ability of the UAS to clean with just cold water. However, the UAS system could work also with chemical cleaners, enabling a synergistic effect of mechanical (acoustically activated bubbles) and chemical cleaning. Furthermore, previous studies have demonstrated that the UAS efficiently removes microbial contamination from rough, etched surfaces, thus demonstrating that UAS has the ability to clean items, such as surgical instruments, that contain dynamic differences in surface topography [40]. In its current form, the UAS system is designed as a hand-held device, and the plan is to include this in a pilot to test as a pre-clean before the surgical instruments proceed on to washer–disinfectors (i.e. at the stage where currently SSDs conduct washing by hand, brushing, and pre-cleaning of surgical instruments). The mechanical removal by UAS of prion-associated amyloid embedded in dried-on brain homogenate demonstrates an interesting parallel with the problem of removing the severe acute respiratory synndrome coronavirus 2 (SARS-CoV-2) virus responsible for the current ccoronavirus disease 19 from touch surfaces. Lacking an appropriate attachment mechanism, the virus relies on the stickiness of respiratory secretions in which it resides (which are composed mainly of mucin glycoproteins, surfactant, and intercellular fluid) to attach to abiotic surfaces. Therefore, the efficient ability of the UAS system for removing prion-associated amyloid by cleaning away the biological material, in the case of this study brain homogenate, as well as bacteria and lubricant contamination, previously published, highlights the importance of testing this system against viruses [40,46]. If viruses can also be removed by UAS, then incorporation of UAS in society to clean these surfaces with just water could aid infection prevention, especially when the use of soap or other cleaning agents is not possible [46]. Prior to the provision of a vaccine, control of an outbreak relies on non-specific measures to break the chain of transmission of the SARS-CoV-2 virus, of which cleaning of solid abiotic surfaces is a vital part.

Although further work is required to confirm the effect of UAS cleaning on prion infectivity, this study has highlighted the

potential of this system as a cheap, rapid, environmentally friendly and highly efficient method for the decontamination of reusable surgical instruments.

Conflict of interest statement

T.G.L. is Director and Inventor-in-Chief of Sloan Water Technology Ltd, which holds the patent to this technology, but has drawn no salary.

Funding sources

This work was supported by the 2011 Royal Society Brian Mercer Award for Innovation, for which the authors are extremely grateful. Time for the study was made available via partial funding from NAMRIP (the Network for Anti-Microbial Resistance and Infection Prevention), which is a University of Southampton Strategic Research Group, and support towards this was received from EPSRC's Network for Antimicrobial Action, 'Bridging the Gap' programme (EP/M027260/1).

References

[1] Bryant G, Hewitt P, Hope J, Howard C, Ironside J, Knight R, et al. Minimise transmission risk of CJD and vCJD in healthcare settings. Report on the Prevention of CJD and vCJD by Advisory Committee on Dangerous Pathogens' Transmission Spongiform Encephalopathy (ACDP TSE) Subgroup. Published as part of the Creutzfeldt–Jakob disease (CJD): guidance, data and analysis reports by the UK. Government Department of Health; 22 October 2015.

[2] Gibbs Jr CJ, Asher DM, Kobrine A, Amyx HL, Sulima MP, Gajdusek DC. Transmission of Creutzfeldt–Jakob disease to a chimpanzee by electrodes contaminated during neurosurgery. J Neurol Neurosurg Psychiatry 1994;57:757–8.

[3] Hervé R, Secker TJ, Keevil CW. Current risk of iatrogenic Creutzfeld–Jakob disease in the UK: efficacy of available cleaning chemistries and reusability of neurosurgical instruments. J Hosp Infect 2010;75:309–13.

[4] Lipscomb IP, Sihota AK, Keevil CW. Diathermy forceps and pencils: reservoirs for protein and prion contamination? J Hosp Infect 2006;64:193–4.

[5] Murdoch H, Taylor D, Dickinson J, Walker JT, Perrett D, Raven NDH, et al. Surface decontamination of surgical instruments: an ongoing dilemma. J Hosp Infect 2006;63:432–8.

[6] Edgeworth JA, Jackson GS, Clarke AR, Weissmann C, Collinge J. Highly sensitive, quantitative cell-based assay for prions adsorbed to solid surfaces. Proc Natl Acad Sci USA 2009;106:3479–83.

[7] Fichet G, Comoy E, Dehen C, Challier L, Antloga K, Deslys JP, et al. Investigations of a prion infectivity assay to evaluate methods of decontamination. J Microbiol Methods 2007;70:511–8.

[8] Flechsig E, Hegyi I, Enari M, Schwarz P, Collinge J, Weissmann C. Transmission of scrapie by steel-surface-bound prions. Mol Med 2001;7:679–84.

[9] Yan ZX, Stitz L, Heeg P, Pfaff E, Roth K. Infectivity of prion protein bound to stainless steel wires: a model for testing decontamination procedures for transmissible spongiform encephalopathies. Infect Control Hosp Epidemiol 2004;25:280–3.

[10] Gill ON, Spencer Y, Richard-Loendt A, Kelly C, Dabaghian R, Boyes L, et al. Prevalent abnormal prion protein in human appendixes after bovine spongiform encephalopathy epizootic: large scale survey. BMJ 2013;347.

[11] Edgeworth JA, Farmer M, Sicilia A, Tavares P, Beck J, Campbell T, et al. Detection of prion infection in variant Creutzfeldt–Jakob disease: a blood-based assay. Lancet 2011;377:487–93.

[12] Hewitt PE, Llewelyn CA, Mackenzie J, Will RG. Creutzfeldt–Jakob disease and blood transfusion: results of the UK Transfusion Medicine Epidemiological Review study. Vox Sang 2006;91:221–30.

[13] Wroe SJ, Pal S, Siddique D, Hyare H, Macfarlane R, Joiner S, et al. Clinical presentation and pre-mortem diagnosis of variant Creutzfeldt–Jakob disease associated with blood transfusion: a case report. Lancet 2006;368:2061–7.

[14] Brown SA, Merritt K, Woods TO, Busick DN. Effects on instruments of the World Health Organization-recommended protocols for decontamination after possible exposure to transmissible spongiform encephalopathy-contaminated tissue. J Biomed Mater Res 2005;72B:186–90.

[15] Dickinson J, Murdoch H, Dennis MJ, Hall GA, Bott R, Crabb WD, et al. Decontamination of prion protein (BSE301V) using a genetically engineered protease. J Hosp Infect 2009;72:65–70.

[16] Edgeworth JA, Sicilia A, Linehan J, Brandner S, Jackson GS, Collinge J. A standardized comparison of commercially available prion decontamination reagents using the Standard Steel-Binding Assay. J Gen Virol 2011;92:718–26.

[17] Fichet G, Antloga K, Comoy E, Deslys JP, McDonnell G. Prion inactivation using a new gaseous hydrogen peroxide sterilisation process. J Hosp Infect 2007;67:278–86.

[18] Lemmer K, Mielke M, Kratzel C, Joncic M, Oezel M, Pauli G, et al. Decontamination of surgical instruments from prions. II. In vivo findings with a model system for testing the removal of scrapie infectivity from steel surfaces. J Gen Virol 2008;89:348–58.

[19] McDonnell G, Burke P. The challenge of prion decontamination. Clin Infect Dis 2003;36:1152–4.

[20] Paspaltsis I, Berberidou C, Poulios I, Sklaviadis T. Photocatalytic degradation of prions using the photo-Fenton reagent. J Hosp Infect 2009;71:149–56.

[21] Secker TJ, Hervé R, Zhao Q, Borisenko KB, Abel EW, Keevil CW. Doped diamond-like carbon coatings for surgical instruments reduce protein and prion-amyloid biofouling and improve subsequent cleaning. Biofouling 2012;28:563–9.

[22] Stephenson J. Halting the spread of human prion disease — exceptional measures for an exceptional problem. J Hosp Infect 2007;2:14–8.

[23] Howlin RP, Khammo N, Secker T, McDonnell G, Keevil CW. Application of a fluorescent dual stain to assess decontamination of tissue protein and prion amyloid from surgical stainless steel during simulated washer–disinfector cycles. J Hosp Infect 2010;75:66–71.

[24] Lipscomb IP, Pinchin H, Collin R, Keevil CW. Effect of drying time, ambient temperature and pre-soaks on prion-infected tissue contamination levels on surgical stainless steel: concerns over prolonged transportation of instruments from theatre to central sterile service departments. J Hosp Infect 2007;65:72–7.

[25] Secker TJ, Hervé R, Keevil CW. Adsorption of prion and tissue proteins to surgical stainless steel surfaces and the efficacy of decontamination following dry and wet storage conditions. J Hosp Infect 2011;78:251–5.

[26] Secker TJ, Pinchin HE, Hervé RC, Keevil CW. Efficacy of humidity retention bags for the reduced adsorption and improved cleaning of tissue proteins including prion-associated amyloid to surgical stainless steel surfaces. Biofouling 2015;31:535–41.

[27] Ungurs M, Hesp JR, Poolman T, McLuckie G, O'Brien S, Murdoch H, et al. Quantitative measurement of the efficacy of protein removal by cleaning formulations; comparative evaluation of prion-directed cleaning chemistries. J Hosp Infect 2010;74:144–51.

[28] Leighton TG, Birkin P, Offin D. A new approach to ultrasonic cleaning. Proc Meet Acoust 2013;19:075029.

[29] Jamaluddin AR, Ball GJ, Turangan CK, Leighton TG. The collapse of single bubbles and approximation of the far-field acoustic emissions for cavitation induced by shock wave lithotripsy. J Fluid Mech 2011;677:305–41.

[30] Leighton TG, Turangan CK, Jamaluddin AR, Ball GJ, White PR. Prediction of far-field acoustic emissions from cavitation clouds during shock wave lithotripsy for development of a clinical device. Proc R Soc Lond A 2013;469:20120538. https://doi.org/10.1098/rspa.2012.0538.
[31] Crawford AE. The measurement of cavitation. Ultrasonics 1964;2:120—3.
[32] Leighton TG, Birkin PR, Hodnett M, Zeqiri B, Power JF, Price GJ, et al. Characterisation of measures of reference acoustic cavitation (COMORAC): an experimental feasibility trial. In: Doinikov AA, editor. Bubble and particle dynamics in acoustic fields: modern trends and applications. Trivandrum, Kerala: Research Signpost; 2005. p. 37—94.
[33] Mason TJ. Ultrasonic cleaning: an historical perspective. Ultrason Sonochem 2016;29:519—23.
[34] Boucher RM, Kreuter J. Measurement of cavitation activity in ultrasonic cleaners. Contam Control 1967;6: 16—18.
[35] Leighton T. Bubble acoustics: from whales to other worlds. Proc Inst Acoustics 2014;36. 58—8.
[36] Maksimov AO, Leighton TG. Transient processes near the threshold of acoustically driven bubble shape oscillations. Acta Acoustica 2001;87:322—32.
[37] Leighton TG. The acoustic bubble: oceanic bubble acoustics and ultrasonic cleaning. Proc Meet Acoustics 2017;24:070006.
[38] Birkin PR, Offin DG, Vian CJB, Leighton TG. Electrochemical 'bubble swarm' enhancement of ultrasonic surface cleaning. Phys Chem Chem Phys 2015;17:21709—15.
[39] Birkin PR, Offin DG, Vian CJB, Howlin RP, Dawson JI, Secker TJ, et al. Cold water cleaning of brain proteins, biofilm and bone — harnessing an ultrasonically activated stream. Phys Chem Chem Phys 2015;17:20574—9.
[40] Howlin RP, Fabbri S, Offin DG, Symonds N, Kiang KS, Knee RJ, et al. Removal of dental biofilms with an ultrasonically activated water stream. J Dental Res 2015;94:1303—9.
[41] Salta M, Goodes L, Maas BJ, Dennington SP, Secker TJ, Leighton TG. Bubbles vs biofilms: a novel method for the removal of marine biofilms attached on antifouling coatings using an ultrasonically activated water stream. Surface Topogr Metrol Prop 2016;4:1—18.
[42] Goodes L, Harvey T, Symonds N, Leighton T. A comparison of ultrasonically activated water stream and ultrasonic bath immersion cleaning of railhead leaf-film contaminant. Surface Topogr Metrol Prop 2016;4:1—10.
[43] Maksimov AO, Leighton TG. Acoustic radiation force on a parametrically distorted bubble. J Acoust Soc Amer 2018;143:296—305.
[44] Costa DdM, Lopes LKdO, Tipple AFV, Johani K, Hu H, Deva AK, et al. Evaluation of stainless steel surgical instruments subjected to multiple use/processing. Infect Dis Health 2018;23:3—9.
[45] Offin DG, Birkin PR, Leighton TG. An electrochemical and high-speed imaging study of micropore decontamination by acoustic bubble entrapment. Phys Chem Chem Phys 2014;16:4982—9.
[46] Malakoutikhah M, Dolder C, Secker T, Zhu M, Harling CC, Keevil C, et al. Industrial lubricant removal using an ultrasonically activated water stream, with potential application for coronavirus decontamination and infection prevention for SARS-CoV-2. Trans Inst Metal Finish 2020;98(5).
[47] Hervé R, Keevil CW. Current limitations about the cleaning of luminal endoscopes. J Hosp Infect 2013;83:22—9.
[48] Saranteas T, Kostopanagiotou GG, Anagnostopoulou S, Mourouzis K, Sidiropoulou T. A simple method for blocking the deep cervical nerve plexus using an ultrasound-guided technique. Anaesth Intens Care 2011;39:971—2.
[49] Lipscomb IP, Herve R, Harris K, Pinchin H, Collin R, Keevil CW. Amyloid-specific fluorophores for the rapid, sensitive in situ detection of prion contamination on surgical instruments. J Gen Virol 2007;88:2619—26.
[50] Hervé R, Collin R, Pinchin HE, Secker T, Keevil CW. A rapid dual staining procedure for the quantitative discrimination of prion amyloid from tissues reveals how interactions between amyloid and lipids in tissue homogenates may hinder the detection of prions. J Microbiol Methods 2009;77:90—7.
[51] Lipscomb IP, Sihota AK, Botham M, Harris KL, Keevil CW. Rapid method for the sensitive detection of protein contamination on surgical instruments. J Hosp Infect 2006;62:141—8.
[52] Keevil CW. Rapid detection of biofilms and adherent pathogens using scanning confocal laser microscopy and episcopic differential interference contrast microscopy. Water Sci Technol 2003;47:105—16.
[53] Leighton TG, Currie HAL, Holgate A, Dolder CN, Jones SL, White PR, et al. Analogies in contextualizing human response to airborne ultrasound and fish response to acoustic noise and deterrents. Proc Meet Acoust 2019;37:010014.
[54] You B, Aubin J-T, Le-Hir G, Arzel A, Laude H, Flan B. In vitro infectivity assay for prion titration for application to the evaluation of the prion removal capacity of biological products manufacturing processes. J Virol Methods 2010;164:1—6.
[55] Stevenson M, Uttley L, Oakley JE, Carroll C, Chick SE, Wong R. Interventions to reduce the risk of surgically transmitted Creutzfeldt—Jakob disease: a cost-effective modelling review. Health Technol Assess 2020;24:11.